North Atlantic Subpolar Gyre Surface Variability (1895-2009)

Gilles Reverdin

North Atlantic Subpolar Gyre Surface Variability (1895–2009)

G. REVERDIN

LOCEAN/IPSL, CNRS/UPMC, Paris, France

(Manuscript received 28 October 2009, in final form 19 April 2010)

ABSTRACT

Surface temperature, salinity, and density are examined in the northeastern part of the North Atlantic subpolar gyre over the last 115 years of measurements. This region presents coherent variability in space but also between different seasons, with relatively small trends and large multidecadal variability. The most significant trend is a lowering in surface density. Multidecadal variability in T and S is large and is usually similar, with the largest difference between the two in the 1920s and a tendency of T to lead S. Multidecadal T and S are correlated with the winter North Atlantic Oscillation (NAO) index at 0 or 1-yr lag for T and 0 to 3-yr lag for S. This suggests a strong contribution of advection. The lag between T and S is also suggestive of a contribution of air–sea fluxes of heat or freshwater, but probably more so at high frequencies than at the multidecadal time scales. Salinity higher frequency is correlated with NAO at a 2–3-yr lag, whereas T higher frequency variability presents no correlation with NAO at any lag. This suggests different relations between seasonal NAO indices and air–sea heat fluxes patterns in this region before and after 1960; also the advective signal is more clearly identified in salinity in this region.

1. Introduction

In recent decades, surface temperature in the North Atlantic subpolar gyre has been shown to respond directly to North Atlantic Oscillation variability as a result of associated heat flux patterns (Visbeck et al. 2003; Hurrell and Deser 2008, among recent papers). Winters with high North Atlantic Oscillation (NAO) index (or more frequent winter occurrence of the NAO+ regime) are known to be associated with large heat loss in the western subpolar gyre and less heat loss in the eastern intergyre region, resulting in increased temperature contrast. It also acts both in phase and with up to 2-yr lag to the subpolar gyre intensity and to the meridional overturning circulations (Eden and Willebrand 2001; Häkkinen 1999; Visbeck et al. 2003). Observations show that the North Atlantic Current (NAC) zonal transport varies as the integral of NAO forcing (Curry and McCartney 2001).

Bersch et al. (2007) comment that the dynamic response to the recent long-term NAO decrease is a southeastward displacement of the subpolar front in the west and a northwestward displacement in the east. This displacement of the front and the associated change in poleward circulation in the eastern part of the gyre is also seen in model results (Herbaut and Houssais 2009; Lohmann et al. 2008). The resulting heat convergence or divergence is thus a strong contributor on yearly or longer time scales to heat content and surface temperature variability in the subpolar gyre (Verbrugge and Reverdin 2003). In addition, there is an Atlantic mode of SST and wind variability associated with multidecadal time scales (AMV) that has a large signature in the subpolar gyre (Kushnir 1994; Ting et al. 2009). It is less understood but could be associated to changes in meridional transport involving the whole Atlantic Ocean.

Salinity variability is less known on those time scales, albeit there has been numerous station data since the 1950s in large parts of the subpolar gyre, which can be used to estimate low-frequency freshwater content signals in the subpolar gyre (Curry and Mauritzen 2005; Boyer et al. 2005) and illustrate decadal variability with a large freshening from 1960 into the early 1990s, followed by a more recent increase (first seen in the surface layers). Near 60°N, air–sea freshwater fluxes explain part of the observed surface salinity variability (between the 1950s and 1998) (Josey and Marsh 2005) but fail to explain the more recent increase that was attributed to advection [for the area near the Reykjanes Ridge cf.

Corresponding author address: G. Reverdin, Laboratoire d'Océanographie et de Climatologie par Expérimentation et Analyse Numérique, Institut Pierre Simon Laplace, Université Pierre et Marie Curie, Case 100, 4 Pl. Jussieu, 75252 Paris CEDEX 05, France.
E-mail: gilles.reverdin@locean-ipsl.upmc.fr

DOI: 10.1175/2010JCLI3493.1

Thierry et al. (2007); for the changes in eastern Atlantic, cf. Hätun et al. (2005) and Frankignoul et al. (2009), mostly from model studies]. Advective signals in the upper layer are also detected mostly along the path of the NAC and its branches in the subpolar gyre from the salinity and temperature variability of 10 yr or less [Belkin et al. (1998) for the Great Salinity Anomalies (GSA); Reverdin et al. (1997); Holliday et al. (2008)], and have also been commented on in model studies by Häkkinen (1993, 2002).

Bersch et al. (2007) summarize some of the changes since the early 1990s in the subpolar gyre and, in particular, the recently well-documented changes related to a decrease of subpolar gyre circulation (Häkkinen and Rhines 2004) since the atmospheric regime shift of 1996 (Cassou et al. 2004). In particular, they outline that initially the meridional near-surface circulation seems to have increased in the eastern Atlantic, as surface density contrast increases initially across the gyre. Then, gradually, as the subpolar gyre retreats and the warmer, saltier waters from the eastern Atlantic invade the central part of the subpolar gyre, this contrast decreases (since 1998, with the largest intrusion of salty water in 2002–04). The recent decades in the eastern part of the North Atlantic subpolar gyre have witnessed nearly in-phase changes between the near surface and intermediate layers (Johnson and Gruber 2007). This hints that, on these decadal time series, surface changes are indicative of large advective changes associated with the ebbing and flowing of more subtropical water to the northern latitudes. Model studies for the late 1950s to the early 2002 period (Hätun et al. 2005; Frankignoul et al. 2009) reinforce this dominant advective source of the variability and relate the recent change to gyre intensity and shape changes. This is also suggested in the long hydrographic time series (Holliday et al. 2008). Holliday (2003) also comment for the Rockall Trough area that a strong contribution of advection led to changes in the surface and intermediate layers between 1970 and 1988; however, the authors did not exclude the possible contribution of local air–sea forcing to these changes, in particular for temperature (Holliday et al. 2000).

The surface waters of the northeastern subpolar gyre are major contributors to the western part of the gyre (Labrador Sea, Irminger Sea) where the deeper waters are formed by winter convection (Lazier 1995; Pickart et al. 2003). Upper-ocean stratification in this region is, however, also strongly influenced at times by inputs of freshwater from the Greenland shelves or flowing from the Arctic into the western Labrador Sea (Yashayaev 2007). This, together with air–sea heat fluxes forcing on surface buoyancy result in the local formation of deeper water being intermittent on an interannual/decadal basis. The seasonal freshening is much smaller east of Greenland in the Irminger Sea, albeit it also happens there—an area less amenable to a large input of freshwater originating from the Arctic. Deep water might also form there at times (Pickart et al. 2003; Vage et al. 2008), but the upper stratification varies from year-to-year so that surface data do not covary closely in relation to what happens below 200–400 m.

Most of this knowledge is gathered from the post-1950 period. SST data portrayed in Kushnir (1994) or more recently in Ting et al. (2009) indicates another multidecadal oscillation with low SSTs in 1905–25, preceded and followed by higher SSTs. NAO-type variability seems to have been less prevalent during these periods (Cassou et al. 2004; Hurrell and van Loon 1997), although Rogers et al. (2004) note increased persistence of the NAO during the early 1920s. Because of these possibly different modes of variability, it is debatable whether the basin-scale response has been similar during that period and in the more recent (1975–95) period of maximum extension of the subpolar gyre, in particular in the eastern subpolar gyre. Surface data are the major source of information on the salinity variability for this earlier period (Reverdin et al. 1994). There is more information on SST, but there are no data in the winter season in a large part of the subpolar gyre before 1920, except in its extreme eastern part and around Iceland (Rayner et al. 2006; Kent and Taylor 2006). Significant effort have been made to homogenize this instrumental SST dataset including mostly bucket and intake measurements until the early 1980s, but uncertainties remain large for this earlier period because of uncertainties on the datasets and the corrections to apply (Kent and Taylor 2006).

Salinity data along 60°N between Greenland and northern Europe presented in Reverdin et al. (2002) outlined long (multidecadal) variability in sea surface salinity (SSS), in addition to short (decadal or less) time scales with apparent similarities between the pre and post 1950 period. The salinity data also presented specific quality problems discussed in Reverdin et al. (1994). The data collected by the Danish operators until 1960, which form a large part of the early dataset on this line (and on a line from Denmark to Iceland), seem to have been usually carefully checked (Knudsen 1905), although at times they present biases (Reverdin et al. 1994). A temperature measurement is almost always associated to the salinity sample. It appears that a large part of these surface data, in particular from the Danish operators before WWI and since 1994, were not incorporated for the Met Office Hadley Centre's sea surface temperature dataset (HadSST2) reanalysis. This

surface dataset from ships of opportunity might provide an alternative to the International Comprehensive Ocean–Atmosphere Dataset (ICOADS) (Worley et al. 2005) to document variability in the North Atlantic subpolar gyre prior to the 1950s.

We will examine the surface temperature and salinity data collected from ships of opportunity or during research cruises so as to investigate the low frequency variability of surface conditions in the eastern part of the North Atlantic subpolar gyre.

2. Datasets

In situ data available before 1992 are described in Reverdin et al. (1994). For the 1895–1960 period, the core of the data in the subpolar gyre originates from the ships of opportunity run under the supervision of the International Council for the Exploration of the Sea (ICES), mostly from Scandinavian countries with a large share of Danish data on the routes from the North Sea to western Greenland (not run in winter before 1945, discontinued in 1910–20 and 1940–45) and Iceland (all year-round, discontinued in 1916–19 and 1940–45). Between the Faroes and Iceland, data from Norwegian sampling is also available in 1931–39, as well as U.K. data in 1896–98, and Swedish data in 1898–99. Close to the Faeroes and west of Scotland, the mix of data is much more complex with additional Swedish and U.K. contributions at different times. In addition, surface data were collected in the 1950–74 period by the weather ships provided by various European countries (mostly by Dutch, U.K., Norwegian, or French ocean weather ships). Since 1994, thermosalinograph (TSG) data are also regularly available (Reverdin et al. 2002). For the period in between, data here are mostly from oceanographic cruises, often from upper levels of CTD or Nansen bottle casts.

These surface data suffer from various instrumental, methodological, and sampling issues, which are reviewed in Reverdin et al. (1994). Different types of draw buckets or intake sampling have been used that result in biases both for temperature (T) (see recent review in Rayner et al. 2006; Kent and Taylor 2006; Smith et al. 2008) and for salinity (S) (Reverdin et al. 1994). Using a draw bucket can have a strong effect on temperature readings (mostly too cold) but also on salinity (too high). The Danish ships consistently used canvas draw buckets (with the exception of the *Ingolf* expedition in 1895–96 with the canvas bucket replaced by an iron bucket most of the time), and this was also the case for U.K. dataset for 1896–98. On the other hand, the water was pumped to draw the water samples for Swedish sampling in 1898–99, but we do not know how temperature was measured. The Norwegian vessels in 1931–39 read temperature from the intake (with a likely positive bias), whereas the water sample was drawn either from the intake or from a small iron bucket. Dutch and French Ocean Weather Ships (OWS), as well as most research vessels (before the 1980s), used a dedicated iron bucket for drawing the water and measuring temperature, whereas on the U.K. OWS *Cumulus* water was drawn (and temperature measured) at the intake.

Biases resulting from the mode of sampling (or storage/analysis of the salinity samples) were documented (for instance, in 1955–60 when the Danish data presented a positive salinity bias of 0.05 compared to nearby U.K. data and were also colder by up to 0.5°C). These biases can be large before 1960 for some of the data, and average biases are estimated based on intercomparison of data from different countries or with bottle data (see Reverdin et al. 1994). These are corrected whenever data origin is identified. However, for part of the data and certain years, the origin of data is not certain so that the corrections applied might not always be adequate. For SST on the Danish vessels, we have adopted a constant correction, based on the comparisons for the period. It is most commonly chosen as 0.2°C, which might be inadequate at times, and is less than what is adopted in HadSST2 for canvas buckets. Our experience with canvas buckets, similar to how the Danish Met Office operated following these recommendations, is that one can obtain in most cases a good reading of SST to within 0.1°C and of salinity to within 0.01 PSS–78 in this region (cf. appendix). However, there is evidence that the canvas buckets in use on Danish merchant vessels were sometimes much smaller than recommended and that the time delay with the bucket on board before reading the temperature was at times much higher (up to 5 min) than what was requested, so errors on temperature and salinity are expected to have been larger than during our investigation (cf. appendix).

The post-1993 TSG data have been first screened to remove data collected with insufficient water flow or contaminated by air bubbles. Then, the salinity data retained were corrected based on water samples regularly drawn at the intake or in a few instances based on nearby near-surface data from validated Argo profiling float profiles. The associated temperature data were either measured at an intake or were measured at the TSG and then corrected based on simultaneous expendable bathythermographs (XBTs). The data needed for the corrections were some times not available or the records uncertain (in particular in the western Irminger Sea), so temperature errors could still be present in these datasets. Despite this, the data quality is certainly much better than for the earlier ships-of-opportunity data.

Possible small (less than 0.1°C) positive temperature biases could be present due either to systematic differences of intake temperature with TSG data or to biases in XBT temperatures used to correct the temperatures (Reverdin et al. 2009). These data also provide much more spatial coverage (most of the different boxes being sampled each month), thus largely reducing the scatter related to poorly sampled spatial variability of the earlier surface data. Other data have been combined to improve sampling, in particular, bottle or CTD data that contribute a good share of the data between 1960 and 2000 near Iceland. Surface data from bottle Nansen casts often needed to be corrected for a small cold surface bias.

As an alternative and to estimate uncertainties due to inhomogeneous spatial sampling, we will use HadSST2 monthly gridded SST fields (Rayner et al. 2006). These analyses are based on the ICOADS 2.0 release (Worley et al. 2005) and include a large number of marine data decks. Although some of the ships used to collect the surface hydrological data also contributed to the marine records, the origin of the temperatures associated to the salinity records and in the marine records is often different. For example, for the U.K. OWS *Cumulus*, unpublished notes [D. Ellett (deceased), personal communication, 1991] comment on the differences between temperature associated with the salinity data and that associated with the meteorological measurements. Thus, to a large extent the two sets are independent, the French or Dutch OWS probably being an exception.

In the analysis presented in section 4, winter NAO index records are used. A station-based index is retained (an extension of the one presented in Hurrell 1995). It has the advantage of being estimated consistently from station data throughout the long period of historical hydrographic data. The results were also checked using a sea level pressure–based index with no significant differences (see discussion in Trenberth and Paolino 1980).

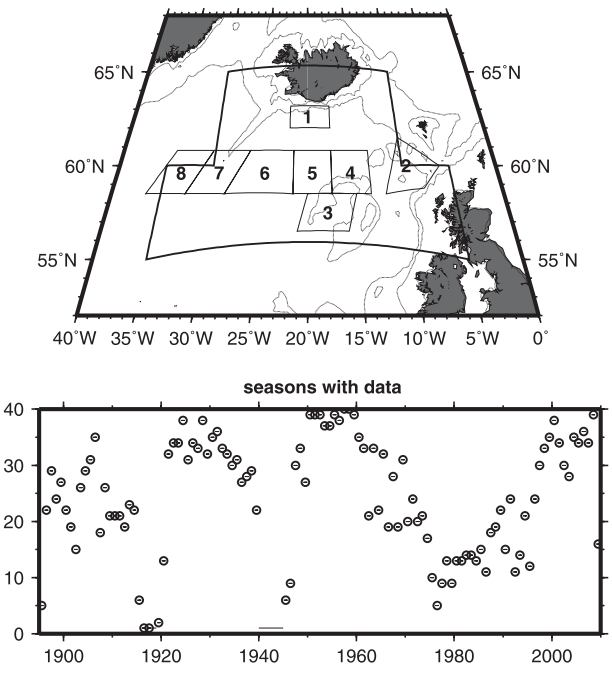

FIG. 1. (top) Map of the area investigated with 200-m, 1000-m-, and 4000-m isobaths plotted. The eight time series are created by combining data within the boxes contoured (light line). The heavy line defines the domain over which HadSST2 fields are averaged to define a regional time series. (bottom) The number of seasons with data summed over the eight time series for each year (out of a total of 40). The five year data gap of World War II is outlined.

3. Time series

a. Methodology

Individual time series are created in eight areas that are relatively well sampled, at least for half of the time between 1895 and 2008, and that cover a large part of the eastern subpolar gyre north of 57°N (mostly the Iceland Basin, as well as the vicinity of the Reykjanes Ridge; Fig. 1). For T in HadSST2, the average of the eight boxes is very close to the spatial average of SST in the subdomain outlined in Fig. 1, which is a reasonably homogeneous region for water mass and salinity (correlation coefficients between the average of the eight time series and the domain time series are larger than 0.98 for all seasons with small rms differences).

First, an average seasonal cycle is removed from the individual data (Reverdin et al. 1994). For salinity, this average seasonal cycle is not always very accurate because of insufficient sampling of large interannual variability. To reduce the effect of errors in the less-well-known salinity seasonal cycle, but to retain enough data, we group the data in five seasons (December–February, March–May, June–July, August–September, and October–November). The first two seasons are longer as they present less variability in the average seasonal cycle, characterized by a net late summer/early autumn decrease on the order of 0.1 PSS-78 (Smed 1943). The winter season (December–February) was only sampled regularly for the area close to southern Iceland (but avoiding the shelves) and the eastern box (areas 1 and 2 in Fig. 1). In other areas, only the four other seasons are sampled. The spring season (March–May) is thus the closest to the late-winter mixing season, and its properties should be close to those of subsurface mode waters formed in late winter.

Then, annual time series are created for each box and each season. A low-pass filtered version is then

produced by filling linearly isolated 1-yr gaps and smoothing by a ¼–½–¼ running mean filter over successive years. This is done for T and S and then a surface density is estimated. Time series are presented as anomalies with respect to the average over the entire time series.

The spring (March–May) time series for southern Iceland presents a typical example (Fig. 2). In this instance, the strongest feature in T and S is the strong dip in 1952, which originates from four data points in early March that we have no reason to disregard. The SST record of the nearby Westmann Islands also indicated low SSTs in early 1952 (Hanna et al. 2006). On the other hand, the large-scale gridded HadSST2 analysis (not shown) does not present this dip. Clearly, spatial sampling was not sufficient at that time to reproduce this larger-scale signal. Errors due to insufficient spatial sampling are not included in our estimation of uncertainty based only on the scatter in the available data, and therefore the estimated uncertainty in the time series is too small for that year (Fig. 2). There are other examples of suspicious year-to-year scatter that could result from insufficient space–time sampling, with a clear improvement toward the end of the time series. The time series of Fig. 2 also suggests variability at decadal or multidecadal time scales both in T and S, but owing to uncertainty resulting from insufficient sampling, they are not well resolved in individual time series. The peak-to-peak range is typically 2°C in T, 0.2 PSS-78 in S, and 0.2 kg m^{-3} in density.

Uncertainties will be reduced by combining time series. When considering temperature from the HadSST2 5° × 5° gridded product, we find high correlation coefficients between the eight different SST time series for the spring season [at least 0.8, with lowest correlation at the easternmost site (box 2)]. For individual boxes, there is a correlation significant at 99% (always greater than 0.6) between time series in spring and in the following June–July season (but less after). These significant correlations also hold for the temperature and salinity time series of our analysis, although the correlation coefficients are smaller, which to a large extent is because of poorer sampling. Averaging the time series of the eight boxes strongly lowers the error resulting from the sampling uncertainties, with an increase of the correlation coefficient for T between our analysis and HadSST2 analysis. Averaging the spring and June–July season further increases this correlation. The time series in the eight boxes have variance increasing from east to west but not substantially. To homogenize the time series we normalize them (to an average standard deviation) before averaging. However, this introduces no significant gain in signal over noise ratio. The uncertainty in the averaged time series for a given year is estimated from the rms deviation between the different time series for that year, when only three or less boxes are combined, and from the uncertainties in the individual time series, when at least four boxes are sampled. We did not statistically fill missing data from the other time series before averaging, and clearly the analysis is less certain when some boxes are not properly sampled. For this reason, we do not keep values for 1917–19 and 1941–44. Also, during 1911–16 and 1945–47, poor data sampling for most time series (except for boxes 1 and 2) results in large uncertainties on the combined time series. This is also the case, but to a lesser degree, during the poor surface sampling from the mid-1970s to mid-1980s or in the 1920s.

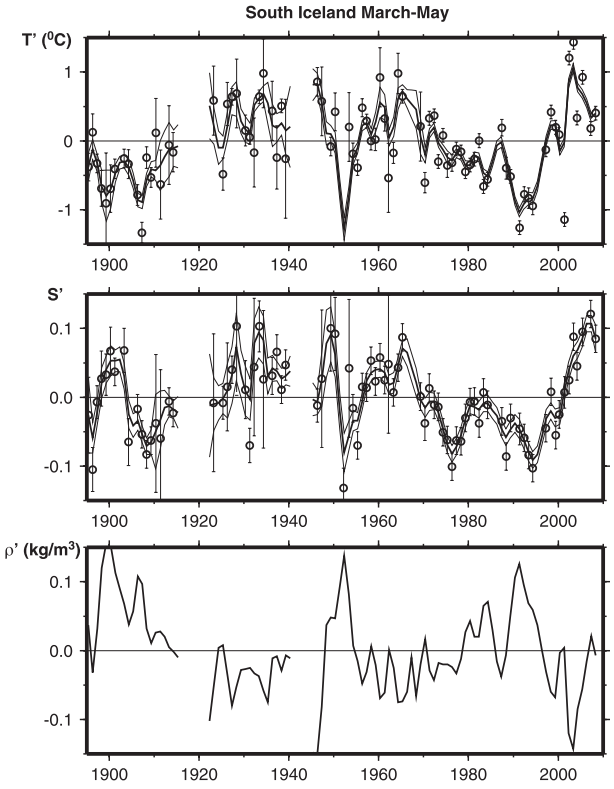

FIG. 2. Time series of temperature, salinity, and density deviations from the average seasonal cycle for area 1 south of Iceland and season March–May. The individual averages are given by dots with the uncertainty on these averages (estimated from the scatter in the individual data) plotted as bars. Time series are plotted with heavy lines, and their standard deviation error range (estimated from the errors on the individual averages, assuming that they are independent) is reported by lighter lines. Uncertainties are not reported on density but have similar magnitudes to what is plotted on temperature.

b. Temperature time series

The resulting temperature time series is highly correlated with the corresponding HadSST2 time series

(correlation coefficient of 0.83 with rms differences of 0.21°C) (Fig. 3). Most features are reproduced, with a few differences, most notably in the late 1920s and for the 1970–90 period when uncertainties are higher. This suggests that sampling might be adequate to investigate multiannual variability, at least for SST after averaging the data to reduce sampling errors. The correlation is actually very similar when considering just the March–May season than when combining the March–May and June–July series. It is also similar when combining four seasons from March to November. However, the variability portrayed is somewhat different during the summer and autumn season, in particular in temperature, so the average of the four seasons is less representative of the hydrographic variability of the upper ocean, which is best identified at the surface at the end of the winter vertical mixing season. To present some general characteristics of the time series, we will thus discuss the average for March–July, this later one presenting slightly smaller uncertainties than for March–May.

To further evaluate the characteristics of our analysis, we will separately depict trends, multidecadal, and higher frequency (HF) variability. The trends are estimated by linear regression. The SST linear trends in this region are not large in both analyses, and therefore the time series is not too sensitive on to how it is removed [here by a linear fit, but see the small differences resulting in adopting a nonlinear trend to model the anthropogenic-induced changes in Ting et al. (2009)]. In the detrended time series, gaps are filled before spectral analysis (for T we chose to replace the gaps by adjusted HadSST2 SST and for S by linear interpolation across the gap). The results are not very sensitive to the way that we fill the gaps, as the two gaps cover less than 7% of the time series length. The spectra of the detrended time series (not shown) present larger energy at multidecadal time scales (periods of 20 yr or longer). This contrasts with the NAO index that, for the same period, presents a slight maximum of energy in the 7–15-yr range within a roughly white spectrum. It might thus be interesting to isolate the higher frequencies (HF) that will be exposed to high NAO forcing from the multidecadal (LF) frequencies. For both T and S, there is an apparent minimum in energy in the 15–18-yr-period range that makes it a suitable cutoff between the two ranges. The separation is chosen at the 18-yr period, with comparable results for other choices of the cutoff in the 12–20-yr range.

First we will further compare this SST product with HadSST2 for the trend and the two spectral ranges, taking the example of the series combining the seasons March–May and June–July. The present analysis presents a larger positive SST trend per century (0.29°C)

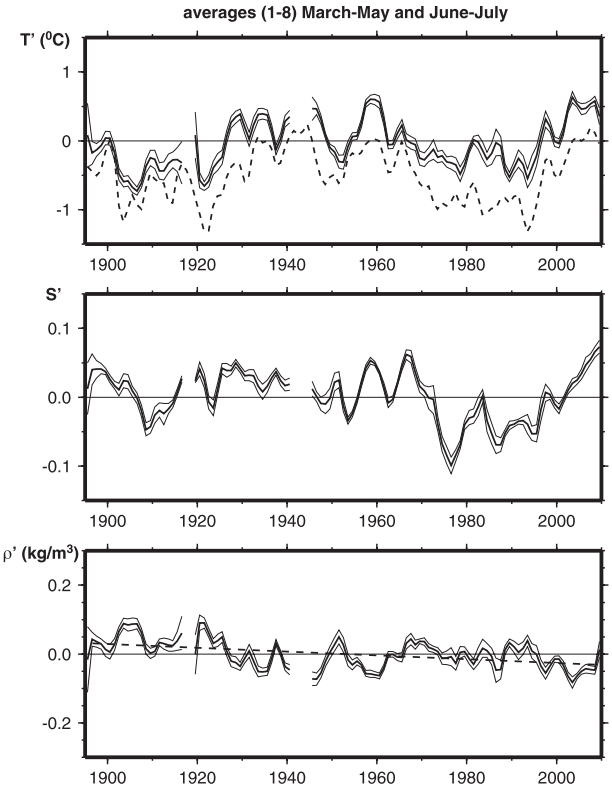

FIG. 3. Combined time series for the eight areas and two seasons, March–May and June–July, of temperature, salinity, and density. The one standard deviation uncertainty on the average is reported as light lines. The dashed line corresponds to (top) temperature from HadSST2 (shifted negatively) and (bottom) the linear trend of density.

than HadSST2 (0.04°C). The trends have large uncertainties related to the variability present in the time series, but the difference between the two time series has much less variability, so the trend of the difference between time series is highly significant (rms error of 0.10°C, the trend is nonzero at the 98% confidence level). This trend originates from lower temperatures in the early part of the twentieth century and higher temperatures since 1994 in this analysis compared to HadSST2. The early period has mostly canvas bucket data, for which we have applied much smaller corrections (0.2°C) than what is done in HadSST2, especially for the season March–May. Adopting this small correction is based on a small number of comparisons with bottle casts, and also on our experience with buckets of the Danish Met Office type (see appendix). The uncertainty in this correction is clearly of the magnitude of the difference. The difference during the last 15 years, when the temperatures used are mostly from intake sensors, remains to be explained (albeit it is smaller than 0.1°C).

The temperature time series both at multidecadal and at higher frequencies are rather similar in our record and HadSST2 (Fig. 4). There is the same general multidecadal variability portrayed in T, with the largest difference in the 1920s (a rms difference of 0.1°C and correlation significant at the 99% confidence level). Our analysis has also slightly smaller rms than HadSST2 (0.27°C compared to 0.32°C). These two differences are much less pronounced for the March–May season than in June–July. The multidecadal temperature time series has well-known low values from 1905 to 1925 and from 1968 to 1998, as in the detrended North Atlantic SST index (a detrended low-pass average of SST between 0°–60°N) (Ting et al. 2009) characterizing the Atlantic multidecadal variability to which this region's low frequency variability is highly correlated. This holds both for our analysis and for the HadSST2 data. The similarity between the two SST analyses with a vastly different dataset, at least before 1940 and since the mid-1970s, reinforces the conclusions one could hold from HadSST2 time series.

HF variability is also portrayed in a similar way in the two analyses of SST (with a correlation coefficient of 0.71 significantly nonzero at the 99% confidence level and very similar rms variability; Fig. 4). The correlation coefficient is less (0.32) (and the differences are larger, not shown) when considering only March–May, probably because of the noise due to the reduced sampling that has the largest impact on the higher frequencies. The HF SST signal has much less variance (by a factor of 2.7, respective rms of 0.27 and 0.16°C for multidecadal and HF ranges when averaging spectra in March–May and June–July) than the multidecadal signal. It seems to have had larger values (and lower frequencies with periods closer to the 18-yr threshold) before 1965 than after. Interestingly, this change occurs at the time when the multidecadal anomalies become negative and also for a period when the winter atmospheric circulation tends to acquire a dominance of NAO+ regimes for the first time in this record (Cassou et al. 2004).

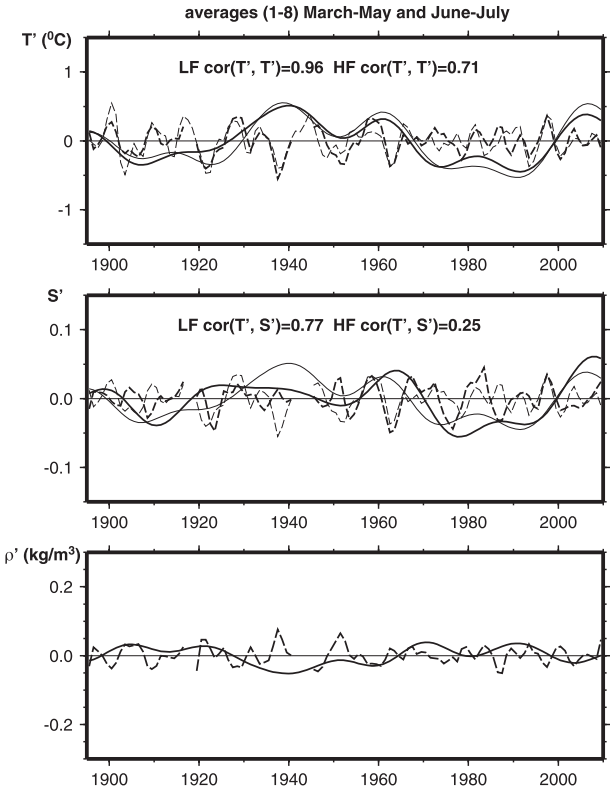

FIG. 4. Multidecadal (full line) and high frequency (HF) (dashed line) components of detrended combined time series for eight areas and seasons March–May and June–July. (top) The heavy line is for this analysis and the light line for HadSST2 SST. (middle) The heavy line is for SSS and the light line for SST, both from this analysis.

c. *Salinity time series*

The salinity time series presents a slight negative trend, -0.028 (100 yr)$^{-1}$. This stands out from the error resulting from the uncertainty on the time series, 0.009 (100 yr)$^{-1}$, but uncertainty on the trend due to the presence of low frequency variability is higher, 0.020 (100 yr)$^{-1}$. The trend found has the same sign and is of similar magnitude in the other seasons, except in October–November when it is smaller, -0.011 (100 yr)$^{-1}$. Furthermore, remaining systematic biases in the data could easily explain differences on the order of 0.02 PSS-78 between the early data and the post-1960 data: we will not comment further on the salinity trend.

The multidecadal signal in salinity appears more energetic by a factor of 2.7 than the higher frequencies (respective rms of 0.028 and 0.017 PSS-78). These higher frequencies present a spike in the 1920s and then larger values from 1950 to 1990, therefore not the same periods as when HF temperature variability was large (except for the 1920 one). The negative deviations for S during the late 1970s and the late 1980s are usually associated with the Great Salinity Anomalies (GSA) (Belkin et al. 1998). This HF variability close to a 10-yr period has also been noticed in hydrographic time series for the period 1950–90 by Reverdin et al. (1997). Interestingly, it does not seem to be present at other times except, maybe, for the early 1920s spike.

The multidecadal low-frequency variability in salinity is correlated with the one in temperature for lags of 0–3 yr (S lagging). [The correlation coefficient of 0.77 at 0 lag is not high, but is significantly positive at the 95% confidence interval considering the small (6) number of

degrees of freedom.] There are some differences in this covariation even for the post-1960 period of better data quality; for instance, the late 1970 low value is more pronounced in salinity. The major difference is, however, from the 1920s to 1950s. In particular, the early 1920s present a positive deviation in S and not in T; however, this is a period with limited sampling (see also the larger differences between the two temperature curves on Fig. 4, top panel).

The higher frequency variability is only marginally correlated between T and S (the correlation coefficient of 0.25 is not significantly positive at the 90% confidence interval for 18 degrees of freedom). In particular, negative S deviations during the late 1970s and the late 1980s associated with the GSAs do not correspond to negative T deviations. The ones in the early 1920s, early 1950s, and early 1960s, on the other hand, also correspond to temperature signals (the last two were also commented on from hydrographic data by Reverdin et al. 1997).

d. Density time series

The density anomalies are dominated in this region by the variability in temperature. It presents a rather large negative trend, -0.065 kg m^{-3} (100 yr)$^{-1}$, with the increases in temperature and decrease in salinity acting in the same direction (Fig. 3). If instead of the temperature trend of our analysis we had used the one in HadSST2, the density trend would have been reduced by 60%. As stated earlier, the salinity trend might also be partially related to methodological considerations. However, the values for both temperature and salinity trends are well above errors related to sampling and random data errors and seem to be above possible method/systematic errors; thus, the negative sign of the density trend is likely to hold for these sources of uncertainty. Furthermore, because the respective contributions of detrended temperature and salinity variability tend to compensate each other partially in density (Fig. 3), the uncertainty of the trend due to density variability is not large, rms error: 0.023 kg m^{-3} (100 yr)$^{-1}$.

In this region, the variability in detrended density presents a larger contribution from (and highly correlated to) temperature than from salinity (roughly by a factor of 2). The combination of the trend and the multidecadal variability produces the lightest surface waters in recent years (2000–08, Fig. 3).

e. Seasonality in deviations from seasonal cycle

The analysis can be done independently for different seasons. The results are presented for our records

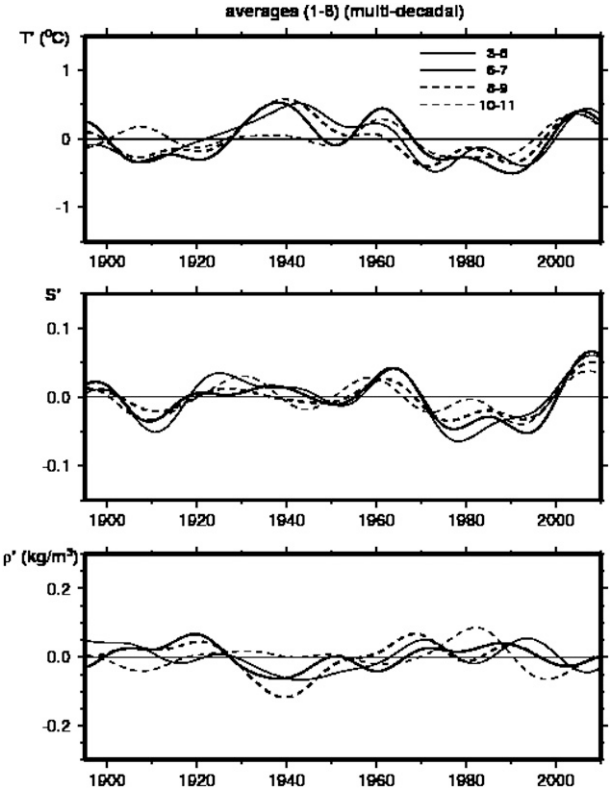

FIG. 5. Multidecadal components of detrended combined time series for four different seasons.

(Fig. 5, multidecadal; Fig. 6, higher frequencies). The multidecadal temperature time series of HadSST2 presents similar features but less difference between the different seasons; in particular, our June–July record seems to differ from HadSST2 in the 1920s and late 1940s—both periods with low sampling and greater uncertainty. In HadSST2, the June–July record is closer to the spring March–May record than what we found (not shown). In both temperature analyses the October–November season presents the largest deviation with other seasons during 1900–50. Otherwise, there is a tendency in T for similar multidecadal signals in the different seasons at least since 1950. For S the different multidecadal time series are even more similar. They diverge most from each other in the 1920s and around 1980. On the other hand, the different multidecadal surface density time series have little in common.

The HF records (Fig. 6) also present some coherence between seasons, although much less so for temperature than for salinity. The HF salinity signals are larger in late summer than in spring. We have to comment, however, that the spring sampling tends to be less adequate for some of the time series than in the summer and late summer periods and that our processing and data

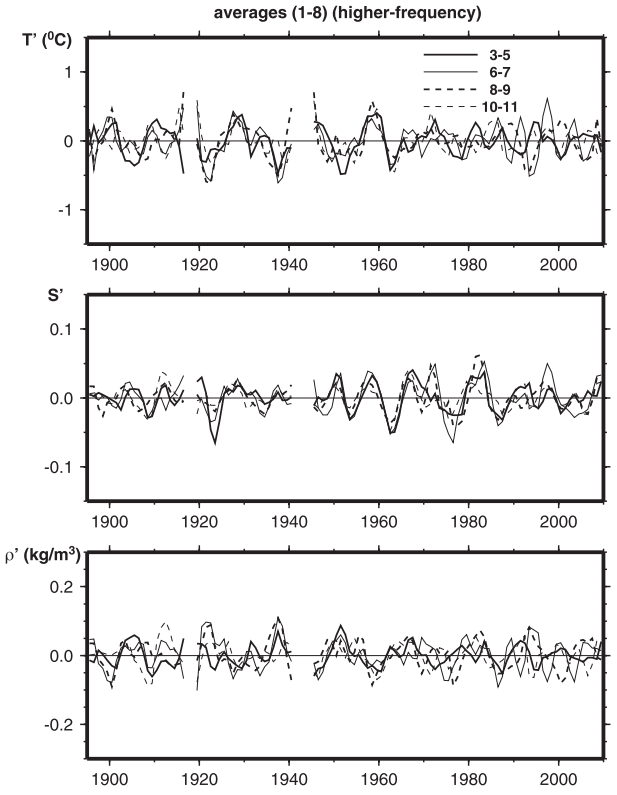

FIG. 6. HF component of detrended combined time series for four different seasons.

smoothing might have reduced the spring higher frequencies more.

4. Discussion and conclusions

a. Trends

The surface time series of T and S originating from hydrographic data are reasonably correlated and can be combined to provide a joint historical record of T, S, and surface density variability in the northeastern part of the North Atlantic subpolar gyre. The trends over the 115 years investigated are relatively small compared to other signals, in particular multidecadal variability. However, they combine to provide a relatively well-defined decrease of surface density in all seasons. This tendency is, however, susceptible to data biases, which we attempted to correct, but could contribute significantly to the density trend, as discussed. Nonetheless, the possibility of a trend toward lower surface density is interesting, as this region is a corridor for waters that later feed into convection regions where some of the world deep-water masses are formed. The lowering of surface water density would, thus, probably affect the properties of newly formed deep water and possibly feedback on the intensity of the meridional overturning circulation in the Atlantic Ocean.

b. The multidecadal records and the 1920s

The multidecadal signals have large variance both for T and S. The multidecadal signal in salinity is correlated to the one in temperature, albeit presenting some differences in the timing and relative amplitudes of different extrema. Changes in the eastward extension of the subarctic front and in the northward penetration of intergyre water are associated with the covariability of T and S. Such changes clearly took place for the well-documented recent positive trend (Bersch et al. 2007; Johnson and Gruber 2007; Häkkinen and Rhines 2009); however, this study suggests that it also took place at other times, for example, around 1910 or in the 1960s and 70s. It could also result from atmospheric forcing.

The difference in the multidecadal T and S for the 1920s (high S but relatively low T) is puzzling, as advective changes for periods of prevailing westerlies are expected to result in covariability. The early 1920s is a period of relatively low sampling and for which there were few comparisons available to correct the surface data (we corrected the Danish S data by -0.05 PSS-78 during 1920–39). The corrections applied are rather uncertain and, although we have no proof for it, it is possible that undetected biases during that period could have resulted in a spurious salinity maximum in the multidecadal records for the 1920s. On the other hand, Cassou et al. (2004) show a different contribution of the climate regimes to this earlier period of prevailing westerly winds than what it was from 1968 to 1995. This could have impacted both heat and freshwater fluxes, and therefore part of the low-frequency response in oceanic surface T and S could be different for that period.

Because of a rather large contribution of higher frequencies to S in the mid-1920s, the time series present a minimum at that time, but not of the same magnitude or duration as in the 1910s (Fig. 3). This is different from what appears in the surface hydrography of the Faroe–Shetland Channel, which presents a very well marked minimum in the mid-1920s (Reverdin et al. 1994; Turrell et al. 1999). However, there too the mid-1920s minimum was preceded and followed quickly by much larger values, so it is not clear if it would project on the multidecadal component. There is also published evidence for a very pronounced salinity minimum in the 1920s farther south in the Rockall Trough (Feni drift, Richter et al. 2009). This suggests a large eastward extension of part of the subpolar front and of the North Atlantic Current toward the Rockall Channel at that time. This is dynamically coherent with the nearly 5-yr high NAO regime (Rogers et al. 2004; Herbaut and Houssais 2009)

but probably not lasting long enough to project onto the multidecadal component. Based on the more recent data, this would be associated temporarily with less penetration of warm and salty water to the subpolar gyre.

c. Higher frequencies

The higher frequencies are less energetic both for T and S than the multidecadal signals. Reverdin et al. (1997) suggested that the different records of surface salinity hydrography in this region are correlated but with some lags of up to 1 yr, probably related to the time scales of advection. The spatial averaging that we did would therefore reduce the amplitude of the higher frequency variability. A ¼–½–¼ filter over successive years was also applied to the time series to smooth the insufficiently resolved interannual variability, so that what is retained is a low-pass version of the interannual to decadal signals. These high-frequency time series are relatively correlated between successive seasons in the year (more so in salinity than temperature). On the other hand, records for T are poorly correlated with records for S.

d. NAO and forcing of surface oceanic signals

To pursue this discussion of differences or similarities between T and S in multidecadal or HF spectral ranges, it is interesting to investigate the relation of these signals with changes of the circulation or air–sea fluxes. This information does not exist reliably over the period sampled, as there were less in situ data to constrain reanalyses (both atmospheric and oceanic), in particular in winters prior to the 1940s. It is commonly accepted that a NAO index is a proxy for the changes in the westerlies across the subpolar gyre, in particular in wintertime. The station-based index has the advantage of homogeneity across the period. It should be related to changes in the westerlies south of 60°N and, thus, result in changes in air–sea fluxes as well as in gyre extension and intensity (Visbeck et al. 2003; Yashayaev et al. 2007; Curry and McCartney 2001). Here, the winter [December–March (DJFM)] NAO index based on station data is retained (Hurrell and van Loon 1997) and is filtered in the same manner as the T and S records.

The fluxes correlated to a positive NAO (see Visbeck et al. 2003 for 1958–2000 estimates) contribute toward a weak oceanic heat loss in this region, whereas they contribute to a clearer freshening. Other contributions to the regional heat and freshwater air–sea fluxes are also important: this is particularly the case for heat fluxes for which the NAO is not a strong contributor in this region. When considering a lagged response because of advection, fluxes in other areas contribute to this forcing. Upstream of this area (farther south or west), NAO-related fluxes clearly contribute to cooling and freshwater fluxes to freshening (including the Ekman contribution). Possible changes of dominant climate regimes (Cassou et al. 2004) could influence the ocean response in T and S, either directly through air–sea fluxes (at 0 lag) or because of low frequency changes in circulation and advection patterns (lagged response).

At multidecadal time scales, a correlation is found (Fig. 7) between the NAO index (-0.25NAO is plotted) and spring temperature (significantly nonzero at the 95% confidence level; this also holds for other seasons). The negative correlation with temperature is maximum with the NAO in the same year (previous winter) or taken with a 1-yr lead. The negative correlation with salinity is maximum for the NAO leading between 0 and 3 yr. The delayed part of the T and S signals could be a response to changes in gyre structure or intensity (as in Curry and McCartney 2001) or advection of anomalies from the western subpolar gyre, as would result from changes in westerlies (NAO). On the other hand, the difference in lags with the NAO for T and S suggest a contribution of forcing by air–sea fluxes but, also, possible damping of SST anomalies by a negative feedback on air–sea fluxes.

The correlation of T or S with the NAO is not significant at 0 lag for HF. More specifically, the record suggests that for SST there might be positive correlation at 0 lag until 1960 and the NAO leading SST by 3 yr after (but with a weak negatively correlated signal). Furthermore, HF S is negatively correlated significantly with the NAO (at the 95% level) when NAO leads by 2–3 yr. This lagged relationship with the NAO index is much less clear in 1985–2000, possibly due to changes in advection time or gyre response, although the propagation of anomalies and changes in gyre structure are clearly seen in hydrographic data for that period (Bersch et al. 2007).

How do we reconcile these differences at HF with the covariability and lagged response to NAO found for T and S at multidecadal time scales? NAO variability has almost as much variance at HF as at multidecadal time scales (by a factor of 1.2), whereas ocean signals were smaller. Thus, at higher frequencies there might be a larger local forcing by air–sea and Ekman fluxes relative to geostrophic advective changes than what is found at the lower frequencies (see also discussion in Krahmann et al. 2001 for the frequency-dependent response in temperature when advection is present). The response of SST to local air–sea fluxes is expected to be large at HF frequencies (Krahmann et al. 2001), whereas Josey and Marsh (2005) commented that from the 1950s to mid-1990s S variability in the northeast Atlantic could be, to some extent, explained by the freshwater fluxes.

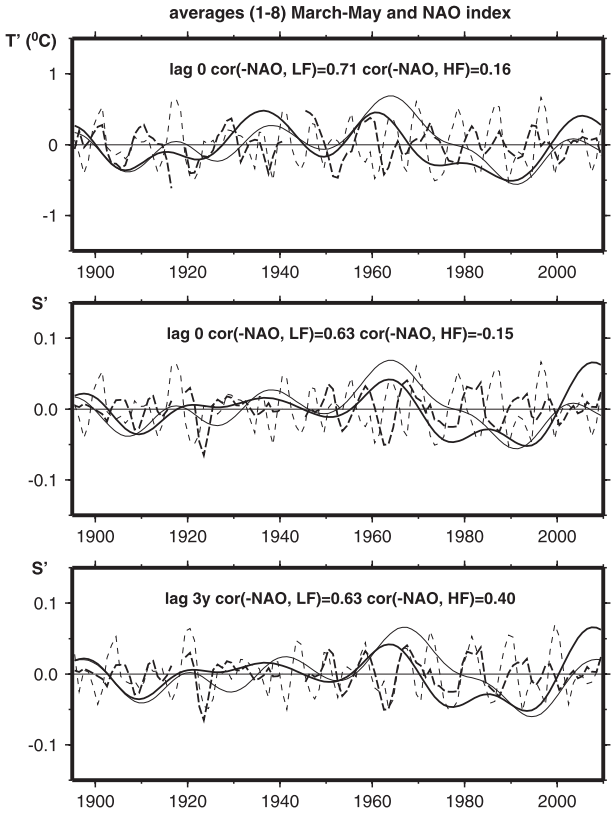

FIG. 7. Multidecadal and HF detrended time series combined for the eight areas and March–May (heavy lines). The light line is for DJFM NAO index (plotted with a reverse sign). (top) For T with the NAO at 0 lag, (middle) for S and NAO at 0 lag, and (bottom) for S and the NAO leading by 3 yr. The correlation coefficients between the NAO index and time series (LF: multidecadal, HF: higher frequencies) are indicated.

However, in this region, freshwater fluxes at the air–sea interface that contribute to S variability are not correlated to the heat fluxes (excluding Ekman advective fluxes) (Josey and Marsh 2005). Furthermore, Thierry et al. (2007) indicated that freshwater air–sea fluxes cannot explain the more recent S variability, with advection and mixing conditions constraining the winter properties in the vicinity of the Reykjanes Ridge. The salinity record also clearly presents some of the GSA signals, in particular in the late 1970s and 1980s, that have been related to outflows of freshwater from the Arctic (Belkin et al. 1998) but are not associated to large temperature signals in the eastern part of the North Atlantic subpolar gyre (Reverdin et al. 1997). The difference between T and S in the HF spectral range thus points to different forcing mechanisms.

e. Mode waters and paleorecords of past variability

Thierry et al. (2007) discussed the variability in mode water formation near the Reykjanes Ridge. These mode waters are one of the precursors to the deep waters formed in the North Atlantic. Surface evolution in T, S and density discussed in this paper for the recent decades is somewhat similar to the signal found in the Reykjanes Ridge mode water formed along the eastern flank of the Reykjanes Ridge. This is not surprising as this mode water is formed in winter by vertical mixing, and we have found that there is a similarity between the salinity time series in different seasons and different sites, so spring season anomalies should be representative of the late winter values. One can thus expect that the records constructed covering the last 115 years also provide indications on the variability of the properties of the mode waters formed in this part of the subpolar gyre. On the other hand, this surface dataset does not provide information on the stratification and volumes of mode water formed, which are a function of local winter conditions (Thierry et al. 2007).

Reconstruction of longer time series of past climate relies on paleorecords. Few have the time resolution relevant for the multidecadal variability that was so prominent in this record. This analysis suggests that poor resolution of these frequencies may not be a major problem in this region, as the largest oceanic signals are multidecadal, at least through the rather short historical record. In this region, the two time series from paleorecords analyzed with nearly sufficient resolution are a record from foraminifer calcite in the Feni drift of Rockall Trough (Richter et al. 2009) and an analysis of alkenone and other sedimentary tracers on the north slope of Iceland (Sicre et al. 2008). The North Iceland record is actually very different from the one in this paper, as it traces Icelandic sea conditions that present little correlations on these time scales with the area south of Iceland investigated here (see also Hanna et al. 2006). The record from the Feni drift (Richter et al. 2009) can be used to investigate changes in water masses in the southern part of the Rockall Trough (near 55°40′N, 14°W) but not so much for spring surface temperature, at least on decadal time scales. Water masses are related to salinity, and this Feni drift record illustrates well the penetration of subpolar gyre water (less saline) in the 1920s and in the 1970s–80s. This seems to be in phase with local records of salinity that are also correlated with the time series from the 1950s to present (Holliday et al. 2008). On the other hand, the 1920s salinity event seems more prominent in the Rockall Trough than in the records presented here (farther west or north). How common are these spatial differences is not known. This could be investigated based on a multiple set of time series over the northeastern part of the subpolar gyre straddling hundreds of years with decadal resolution. This emphasizes the

need for further analysis of proxy records, maybe using deep-sea corals.

Acknowledgments. We are indebted to the valuable collection effort carried under the supervision of ICES for more than a hundred years and to efforts from various individuals to continue the collection and validation of data (special mention to Hedinn Valdimarsson and Magnus Danielsen in Reykjavik, Lars Heilman in Nuuk, and Are Olsen in Bergen, who provided important validation data to correct the recent data from the merchant vessels, and to Denis Diverres from IRD, Dan Smith, and Jack Jossi from NOAA/NMFS for servicing the different ships). The thermosalinograph data used here since 1994 were mostly acquired with support of ORE SSS (Toulouse, France), US191 of IRD (Brest, France), and NOAA (both NMFS in Narragansett and AOML in Miami). Helpful comments on the manuscript were received from Penny Holliday, Elizabeth Kent, and Christophe Herbaut, as well as from three reviewers. Financial support from INSU to ORE SSS and to the OVIDE project of LEFE, from ANR Newton, and from FP7 Grant THOR is gratefully acknowledged.

APPENDIX

Bucket Sampling on Merchant Vessels

A canvas draw bucket was tested on the voluntary observing ship (VOS) *Skogafoss* during three crossings in June 1993, January, and April 1994 between Iceland and Newfoundland. This large canvas bucket (U.K. meteorological model) is very similar to the one recommended by the Danish Meteorological Office for their observing vessels until the 1970s. The bucket was plunged, usually twice (weather permitting), from the side (back) of the ship and hauled back after one minute and placed in a relatively protected part of the deck. Measurement of T was usually made within two minutes and the salinity sample was drawn afterward from the same bucket (some times drawn after refilling the bucket). Other salinity samples were often collected from a ship intake faucet, and temperature was also measured from an intake sensor during the April 1994 cruise.

The positive salinity biases of samples drawn from the bucket (compared to intake samples) were usually smaller than 0.01 PSS-78, with an average difference/scatter of 0.006 (0.02) PSS-78 in January 1994. If this was due to evaporation, this would be associated with a small cooling of the bucket. This evidence and also the small evolution observed between successive readings of bucket temperature at 3′ latitude intervals, we estimate that the error should have been less than 0.1°C (winds were force 7–10 (Beaufort scale), but the bucket was usually well protected from the wind). Out of 74 measurements in April 1994, 71 present deviations less than 0.2°C to the intake temperature, with average deviation (scatter) of −0.01°C (0.12°C). The bucket temperature cold bias might be larger as there could be ocean stratification at the time, so the in situ temperature of the water collected in the bucket could be a little higher than the intake temperature. The three other values for that crossing that were measured at wind force 8 and the bucket fairly exposed to the wind present much larger negative biases, at least −0.3°C. Averaged over the whole crossing, the errors in these three nonoptimal measurements result in an average additional −0.02°C bias. Altogether, for that cruise too, the average T bias is likely to have been less than −0.1°C.

These measurements with a bucket, during very good operating conditions provide some indications of what the minimum biases are with a canvas draw bucket collection in the often severe conditions encountered in the North Atlantic subpolar gyre. It is quite likely that the way the bucket was used was not always favorable and that the canvas bucket was not always as large as the recommended bucket size on Danish vessels. This would result in larger errors both for T and S. Based on comparisons between ship and station data, we estimate that the temperature error was at least −0.2°C (Reverdin et al. 1994). This minimal bias estimate is what we retained for correcting the temperature observations from the Danish merchant vessels.

REFERENCES

Belkin, I. M., S. Levitus, J. Antonov, and S.-A. Malmberg, 1998: ''Great salinity anomalies'' in the North Atlantic. *Prog. Oceanogr.,* **41,** 1–68.

Bersch, M., I. Yashayaev, and K. P. Koltermann, 2007: Recent changes of the thermohaline circulation in the subpolar North Atlantic. *Ocean Dyn.,* **57,** 223–235.

Boyer, T., S. Levitus, J. Antonov, R. Locarnini, A. Mishonov, H. Garcia, and S. A. Josey, 2005: Changes in freshwater content in the North Atlantic Ocean 1955–2006. *Geophys. Res. Lett.,* **34,** L16603, doi:10.1029/2007GL030126.

Cassou, C., L. Terray, J. W. Hurrell, and C. Deser, 2004: North Atlantic winter climate regimes: Spatial asymmetry, stationarity with time, and oceanic forcing. *J. Climate,* **17,** 1055–1068.

Curry, R. G., and M. S. McCartney, 2001: Ocean gyre circulation changes associated with the North Atlantic Oscillation. *J. Phys. Oceanogr.,* **31,** 3371–3400.

——, and C. Mauritzen, 2005: Dilution of the northern North Atlantic Ocean in recent decades. *Science,* **308,** 1772–1774.

Eden, C., and J. Willebrand, 2001: Mechanism of interannual to interdecadal variability of the North Atlantic circulation. *J. Climate,* **14,** 2266–2280.

Frankignoul, C., J. Deshayes, and R. Curry, 2009: The role of salinity in the decadal variability of the North Atlantic meridional overturning circulation. *Climate Dyn.,* **33,** 777–793.

Häkkinen, S., 1993: An Arctic source for the Great Salinity Anomaly: A simulation of the Arctic ice ocean system for 1955–1975. *J. Geophys. Res.,* **98,** 16 397–16 410.

——, 1999: Variability of the simulated meridional heat transport in the North Atlantic for the period 1951–1993. *J. Geophys. Res.,* **104,** 10 991–11 007.

——, 2002: Surface salinity variability in the northern North Atlantic during recent decades. *J. Geophys. Res.,* **107,** 8003, doi:10.1029/2001JC000812.

——, and P. Rhines, 2004: Decline of subpolar North Atlantic circulation during the 1990s. *Science,* **304,** 555–559.

——, and ——, 2009: Shifting surface currents in the northern North Atlantic Ocean. *J. Geophys. Res.,* **114,** C04005, doi:10.1029/2008JC004883.

Hanna, E., T. Jonsson, J. Olafsson, and H. Valdimarsson, 2006: Icelandic coastal sea surface temperature records reconstructed: Putting the pulse on air–sea–climate interactions in the northern North Atlantic. Part I: Comparison with HadISST1 open-ocean surface temperatures and preliminary analysis of long-term patterns and anomalies of SSTs around Iceland. *J. Climate,* **19,** 5652–5666.

Hätun, H., A. B. Sando, H. Drange, B. Hansen, and H. Valdimarsson, 2005: Influence of the Atlantic subpolar gyre on the thermohaline circulation. *Science,* **309,** 1841–1844.

Herbaut, C., and M.-N. Houssais, 2009: Response of the eastern North Atlantic subpolar gyre to the North Atlantic Oscillation. *Geophys. Res. Lett.,* **36,** L17607, doi:10.1029/2009GL039090.

Holliday, N. P., 2003: Air–sea interaction and circulation changes in the northeast Atlantic. *J. Geophys. Res.,* **108,** 3259, doi:10.1029/2002JC001344.

——, R. T. Pollard, J. F. Read, and H. Leach, 2000: Water mass properties and fluxes in the Rockall Trough: 1975 to 1998. *Deep-Sea Res. I,* **47,** 1303–1332.

——, and Coauthors, 2008: Reversal of the 1960s to 1990s freshening trend in the northeast North Atlantic and Nordic Seas. *Geophys. Res. Lett.,* **35,** L03614, doi:10.1029/2007GL032675.

Hurrell, J. W., 1995: Decadal trends in the North Atlantic Oscillation: Regional temperatures and precipitation. *Science,* **269,** 676–679.

——, and H. van Loon, 1997: Decadal variations in climate associated with the North Atlantic Oscillation. *Climatic Change,* **36,** 301–326.

——, and C. Deser, 2008: North Atlantic climate variability: The role of the North Atlantic Oscillation. *J. Mar. Syst.,* **78,** 28–41.

Johnson, G. C., and N. Gruber, 2007: Decadal water mass variations along 20°W in the northeastern Atlantic Ocean. *Prog. Oceanogr.,* **73,** 277–295.

Josey, S. A., and R. Marsh, 2005: Surface freshwater flux variability and recent freshening of the North Atlantic in the eastern subpolar gyre. *J. Geophys. Res.,* **110,** C05008, doi:10.1029/2004JC002521.

Kent, E., and P. K. Taylor, 2006: Toward estimating climatic trends in SST. Part I: Methods of measurement. *J. Atmos. Oceanic Technol.,* **23,** 464–475.

Knudsen, M., 1905: Contribution to the hydrography of the North Atlantic Ocean. *Meddelelser fra Kommissionen for Havundersogelser. Serie Hydrographi,* No. 6, Copenhagen, 1–34.

Krahmann, G., M. Visbeck, and G. Reverdin, 2001: Formation and propagation of temperature anomalies along the North Atlantic Current. *J. Phys. Oceanogr.,* **31,** 1287–1303.

Kushnir, Y., 1994: Interdecadal variations in North Atlantic sea surface temperature and associated atmospheric conditions. *J. Climate,* **7,** 141–157.

Lazier, J. R. N., 1995: The salinity decrease in the Labrador Sea over the past thirty years. *Natural Climate Variability on Decade-to-Century Time Scales,* National Academy Press, 295–304.

Lohmann, K., H. Drange, and M. Bentsen, 2008: Response of the North Atlantic subpolar gyre to persistent North Atlantic oscillation like forcing. *Climate Dyn.,* **32,** 273–285.

Pickart, R. S., F. Straneo, and G. W. K. Moore, 2003: Is Labrador Sea water formed in the Irminger Basin? *Deep-Sea Res. I,* **50,** 23–52.

Rayner, N. A., P. Brohan, D. E. Parker, C. K. Folland, J. J. Kennedy, M. Vanicek, T. J. Ansell, and S. F. B. Tett, 2006: Improved analyses of changes and uncertainties in sea surface temperature measured in situ since the mid-nineteeth century: The HadSST2 dataset. *J. Climate,* **19,** 446–469.

Reverdin, G., D. Cayan, H. D. Dooley, D. J. Ellett, S. Levitus, Y. du Penhoat, and A. Dessier, 1994: Surface salinity of the North Atlantic: Can we reconstruct its fluctuations over the last one hundred years? *Prog. Oceanogr.,* **33,** 303–346.

——, ——, and Y. Kushnir, 1997: Decadal variability of hydrography in the upper northern North Atlantic 1948–1990. *J. Geophys. Res.,* **102,** 8505–8531.

——, F. Durand, J. Mortensen, F. Schott, H. Valdimarsson, and W. Zenk, 2002: Recent changes in the surface salinity of the North Atlantic subpolar gyre. *J. Geophys. Res.,* **107,** 8010, doi:10.1029/2001JC001010.

——, F. Marin, B. Bourlès, and P. L'Herminier, 2009: XBT temperature errors during French research cruises (1999–2008). *J. Atmos. Oceanic Technol.,* **26,** 2462–2473.

Richter, T. O., F. J. C. Peeters, and T. C. E. van Weering, 2009: Late Holocene (0-2.4 ka BP) surface water temperature and salinity variability, Feni Drift, NE Atlantic Ocean. *Quat. Sci. Rev.,* **28,** 1941–1955.

Rogers, J. C., S. H. Wang, and D. H. Bromwich, 2004: On the role of the NAO in the recent northeastern Atlantic arctic warming. *Geophys. Res. Lett.,* **31,** L02201, doi:10.1029/2003GL018728.

Sicre, M. A., and Coauthors, 2008: A 4500-year reconstruction of sea surface temperature variability at decadal time-scales off North Iceland. *Quat. Sci. Rev.,* **27,** 2041–2047.

Smed, J., 1943: Annual and seasonal variations in the salinity of the North Atlantic surface water. *Rapports et Procès-Verbaux des Reunions,* Vol. 112, International Council for the Exploration of the Sea, 77–94.

Smith, T. M., R. W. Reynolds, T. C. Peterson, and J. Lawrimore, 2008: Improvements to NOAA's historical merged land–ocean surface temperature analysis (1880–2006). *J. Climate,* **21,** 2283–2296.

Thierry, V., E. de Boisséson, and H. Mercier, 2007: Rapid changes in the properties of the Reykjanes Ridge mode waters over 1990–2006. *J. Geophys. Res.,* **113,** C04016, doi:10.1029/2007JC004443.

Ting, M., Y. Kushnir, R. Seager, and C. Li, 2009: Forced and internal twentieth-century SST trends in the North Atlantic. *J. Climate,* **22,** 1469–1481.

Trenberth, K. E., and D. A. Paolino Jr., 1980: The Northern Hemisphere sea level pressure data set: Trends, errors, and discontinuities. *Mon. Wea. Rev.,* **108,** 855–872.

Turrell, W. R., G. Slesser, R. D. Adams, R. Payne, and P. A. Gillibrand, 1999: Decadal variability in the composition of Faroe Shetland Channell. *Deep Sea Res. I,* **46,** 1–25.

Vage, K., and Coauthors, 2008: Surprising return of deep convection to the subpolar North Atlantic Ocean in winter 2007–2008. *Nat. Geosci.,* **2,** 67–72.

Verbrugge, N., and G. Reverdin, 2003: Contribution of horizontal advection to the interannual variability of sea surface temperature in the North Atlantic. *J. Phys. Oceanogr.,* **33,** 964–978.

Visbeck, M., E. P. Chassignet, R. G. Curry, T. L. Delworth, R. R. Dickson, and G. Krahmann, 2003: The ocean's response to North Atlantic Oscillation variability. *The North Atlantic Oscillation: Climatic Significance and Environmental Impact, Geophys. Monogr.,* Vol. 134, Amer. Geophys. Union, 113–145.

Worley, S. J., S. D. Woodruff, R. W. Reynolds, S. J. Lubker, and N. Lott, 2005: ICOADS Release 2.1 data and products. *Int. J. Climatol.,* **25,** 823–842.

Yashayaev, I., 2007: Hydrographic changes in the Labrador Sea, 1960–2005. *Prog. Oceanogr.,* **73,** 242–276.